MATHEMATICA MONTISNIGRI
Vol XXVII (2013) 53-63

LOCAL TWO-DIMENSIONAL PERTURBATIONS EVOLUTION IN SMALL-CONDUCTIVITY GAS FLOW IN MAGNETIC FIELD

A. GALANINA, A. FAVORSKIY

Lomonosov Moscow State University
Moscow, Russia
e-mail: galaninaanna@gmail.com

Summary. The work is dedicated to the numerical solution of T-layer development from local temperature perturbations in small-conductivity gas flow. The problem is two-dimensional. The impact of perturbation of initial parameters on T-layer development and stability is investigated.

1 INTRODACTION

In the beginning of 1970, during the numerical solution of some class of magnetic hydrodynamics problems the T-layer effect was discovered. The T-layer is a high-temperature self-sustaining area in plasma moving in a magnetic field. The T-layer derivation is caused by nonlinear connections between electromagnetic and gasdynamic plasma parameters. Conditions of derivation, evolution and stability of this phenomenon for one-dimensional task are rather fully studied and described in work[1]. Preprint[2] is dedicated to the theoretical research of temperature growth evolution to stable mode possibility in case of additional mechanisms of energy outlet. The work[3] is devoted to the two-dimensional problem of T-layer evolution. In this work it is shown that in specific problem definition initially two-dimensional flow structure reconstructs during the time and finally becomes one-dimensional (the solution does not depend on the second spatial coordinate while the initial conditions significantly depend on it).

This work is dedicated to further research of T-layer derivation and evolution conditions for two-dimensional problem. The impact of temperature perturbation of initial parameters and the flow characteristics is investigated. The numerical solution algorithm is based on quasiacoustic scheme[4].

2 PROBLEM DEFINITION

Let's consider the two-dimensional flat channel on *(x, y)* coordinate plane with constant width D (along y axis) filled with homogeneous compressible gas moving along channel axis (x axis). The gas conductivity that depends on its temperature is not enough for making gas interact with the magnetic field. At the initial moment of time the magnetic field is homogeneous and has only one non-zero component directed along z-direction. Nonperturbed initial temperature is equal to T_0. At the initial time moment $t=0$ a local temperature perturbation up to value $T_1 > T_0$ is introduced into the gas flow. Due to this gas conductivity also increases and becomes enough significant to provide gas and magnetic field interaction. We are interested in this perturbation further development in time and space (fig. 1).

2010 Mathematics Subject Classification: 65C20, 97M50, 78A25.
Key words and Phrases: Math simulation, Magnetohydrodynamics, Magnetic field, Small-conductivity gas, T-layer

Note that domain inside channel can be also considered as an element of periodically perturbed flow structure with period D along y-direction.

For this problem let us use magnetohydrodynamics system of equations for plane flow in Euler coordinates:

$$\begin{cases} \dfrac{\partial \rho}{\partial t}+\dfrac{\partial \rho u}{\partial x}+\dfrac{\partial \rho v}{\partial y}=0; \\ \dfrac{\partial \rho u}{\partial t}+\dfrac{\partial}{\partial x}\left(p+\dfrac{H^2}{8\pi}+\rho u^2\right)+\dfrac{\partial \rho uv}{\partial y}=0; \\ \dfrac{\partial \rho v}{\partial t}+\dfrac{\partial \rho uv}{\partial x}+\dfrac{\partial}{\partial y}\left(p+\dfrac{H^2}{8\pi}+\rho v^2\right)=0; \\ \dfrac{\partial}{\partial t}\left[\rho\left(\varepsilon+\dfrac{u^2+v^2}{2}\right)\right]+\dfrac{\partial}{\partial x}\left[\rho u\left(\varepsilon+\dfrac{p}{\rho}+\dfrac{u^2+v^2}{2}\right)\right]+\dfrac{\partial}{\partial y}\left[\rho v\left(\varepsilon+\dfrac{p}{\rho}+\dfrac{u^2+v^2}{2}\right)\right]= \\ =\dfrac{1}{4\pi}\left[\left(\dfrac{c^2}{4\pi\sigma}\dfrac{\partial H}{\partial x}-uH\right)\dfrac{\partial H}{\partial x}+\left(\dfrac{c^2}{4\pi\sigma}\dfrac{\partial H}{\partial y}-vH\right)\dfrac{\partial H}{\partial y}\right]; \\ \vec{j}=\dfrac{c^2}{4\pi}\operatorname{rot}\vec{H}, \quad \dfrac{1}{c}\dfrac{\partial \vec{H}}{\partial t}=\dfrac{1}{c}\operatorname{rot}\left[\vec{V}\times\vec{H}\right]-\operatorname{rot}\vec{E}, \quad \operatorname{div}\vec{H}=0, \quad \vec{j}=\sigma\vec{E} \end{cases} \tag{1}$$

(here t is time, ρ is density, $\vec{V}=(u, v, 0)$ is velocity vector, p is pressure, ε is specific bulk internal energy, $\vec{H}=(0, 0, H)$ is the magnetic field strength, $\vec{E}=(E_x, E_y, 0)$ is the electric field strength, $\vec{j}$ is the current density, σ is gas conductivity). In addition let's assume that the gas is described by ideal polytrophic gas state equation. The gas conductivity σ is a power function of gas temperature:

$$\sigma=\sigma_0\left(\frac{T}{T_0}\right)^{\alpha}, \quad \alpha>0, \tag{2}$$

which is characteristic for low-temperature plasma[3].

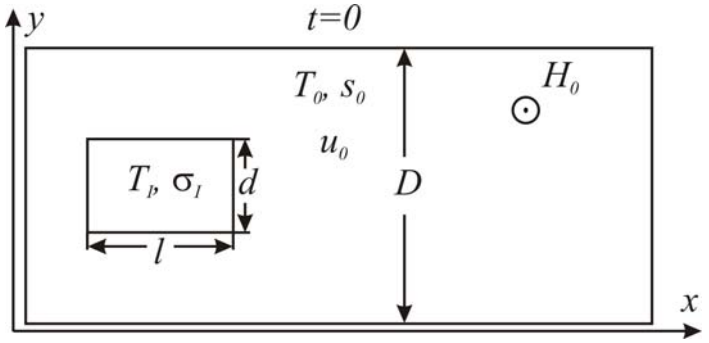

Figure 1. Problem setup

Consider initially supersonic flow with Mach number $M=2,66$. At the initial time moment the temperature perturbation is a rectangular domain in (x, y) plane with length l and width d

(fig. 1). Let term the ratio between perturbation width and channel width *d/D* as on-off time ratio and study the possibility of T-layer evolution in dependence of this ratio value. Magnetic field on the right boundary $x=L$ is maintained constant, on the left boundary $x=0$ it is assumed that $E_y=0$, on the horizontal boundaries $E_x=0$.

3 NUMERICAL SOLUTION ALGORITHM

For the formulated problem the splitting on physical processes method[4] is used. As a result the numerical solution of this equations system is divided into three stages. The first stage is the system gasdynamic parameters calculation at new time layer without interaction with the magnetic field (the first four equations in the system (1)). The second stage is the electromagnetic parameters computation (the last equation in the system (1)). Finally, gasdynamic parameters are recalculated considering the electromagnetic interaction.

3.1 Gasdynamic parameters computation in Lagrange coordinates

Let's consider quasiacoustic scheme[5] construction and its main features. This scheme is used for the parameter calculation on the first stage of numerical algorithm for T-layer problem. To make it more demonstrative we explain scheme construction for the one-dimensional problem. Then we show how this algorithm can be transformed for the two-dimensional problem.

So on the first stage the gas dynamic equation system is solved without electromagnetic interaction. The numerical algorithm for this system solution is also divided into two substages. At first we find the solution of system in Lagrange variables. Then we recalculate the obtained solution into Euler coordinates. This algorithm allows better reproduction of contact and tangential shocks.

The coordinate ξ of particle initial position at zero time moment is defined as Lagrange spatial variable, i. e. $x(0)=\xi$. The gas dynamic equation system in Lagrange coordinates for one-dimensional plane flow in conservative form is as follows[6]:

$$\begin{cases} \dfrac{\partial}{\partial t}\left(\dfrac{\rho^0(\xi)}{\rho}\right)=\dfrac{\partial u}{\partial \xi}; \\ \dfrac{\partial}{\partial t}\left(\rho^0(\xi)u\right)+\dfrac{\partial p}{\partial \xi}=0; \\ \dfrac{\partial}{\partial t}\left(\rho^0(\xi)\left[\varepsilon+\dfrac{u^2}{2}\right]\right)+\dfrac{\partial pu}{\partial \xi}=0; \end{cases} \tag{3}$$

here $\rho^0(\xi)$ is the density function at the initial time moment. The numerical solution of this problem is constructed in mesh function class with the uniform grid with nodes (ξ_k,t_j), where $\xi_k=\xi_1+kh$, $k=0,1,\ldots,N$; $t_j=j\tau$, $j=0,1,\ldots, J$; N is the total number of special cells ; $h=(\xi_2-\xi_1)/N$ is the constant spatial step; τ is constant time step.

The integro-interpolation method[4] (or balance method or finite-volume method) is used for difference scheme construction. After each of the system equations is integrated over the space-time cell the conversation lows of mass, momentum and energy arise:

$$\begin{cases} \Delta x_k^{j+1} - \Delta x_k^j = WUI_{k+1/2}^j - WUI_{k-1/2}^j, \\ h\left(q_k^{j+1} - q_k^j\right) + WQI_{k+1/2}^j - WQI_{k-1/2}^j = 0, \\ h\left(e_k^{j+1} - e_k^j\right) + WEI_{k+1/2}^j - WEI_{k-1/2}^j = 0, \end{cases} \tag{4}$$

here Δx_k^j is the particle volume, q_k^j is momentum and e_k^j is the volume average energy value in grid cell. Addendums $WUI_{k+1/2}^j$, $WQI_{k+1/2}^j$ and $WEI_{k+1/2}^j$ are the integral flows of the corresponding functions evaluated at the intercell boundaries over the time τ.

Let's determine on each segment $[\xi_{k-1/2},\xi_{k+1/2}]$ the local linear spline interpolation of functions ρ, u and p at time moment $t=t_j$ as follows:

$$f_k(\xi, t_j) = f_k^j + D_k^j\left(\xi - \xi_k\right), \tag{5}$$

here $f=\rho$, $f=u$ or $f=p$. Spline coefficient D_k^j is defined as

$$D_k^j = \frac{\left|f_{\xi}^j\right| f_{\bar{\xi}}^j + \left|f_{\bar{\xi}}^j\right| f_{\xi}^j}{\left|f_{\xi}^j\right| + \left|f_{\bar{\xi}}^j\right|}, \tag{6}$$

where f_{ξ}^j and $f_{\bar{\xi}}^j$ are forward and backward approximations to space derivative.

This choice of D_k^j provides the monotone of local linear spline function $f_k(\xi,t_j)$ if mesh function $\{f_k^j\}$ is monotonous.

On each segment $[\xi_k,\xi_{k+1}]$ the linear spline-functions $f_k(\xi,t_j)$ and $f_{k+1}(\xi,t_j)$ are divided into a set of horizontal layers enumerated with $m=1,\ldots,M$. This layers are parallel to the abscissa axis (fig. 2, a). The number of layers M is chosen so that the layers are small enough and can be defined as small disturbances.

Let's distinguish a horizontal layer that is the nearest to the average value between spline-functions $f_k(\xi_{k+1/2},t_j)$ and $f_{k+1}(\xi_{k+1/2},t_j)$ values at the intercell boundary $\xi=\xi_{k+1/2}$ (fig. 2, a). This layer we determine as the common constant background for function f between this two cells. We denominate it as $f_{F,k+1/2}$.

Each of spline-functions $f_k(\xi,t_j)$ and $f_{k+1}(\xi,t_j)$ in half-cells $[\xi_k,\xi_{k+1/2}]$, $[\xi_{k+1/2},\xi_{k+1}]$ is replaced with a construction shown on figure 2, a. This construction consists of the common constant background $f_{F,k+1/2}$ and small disturbances rectangular "bricks" that "lie" on the background (taking into account disturbance sign). It is important that every "brick" has its own individual background. It is either common constant background $f_{F,k+1/2}$ or another "brick" that adjoin it from the side of constant background.

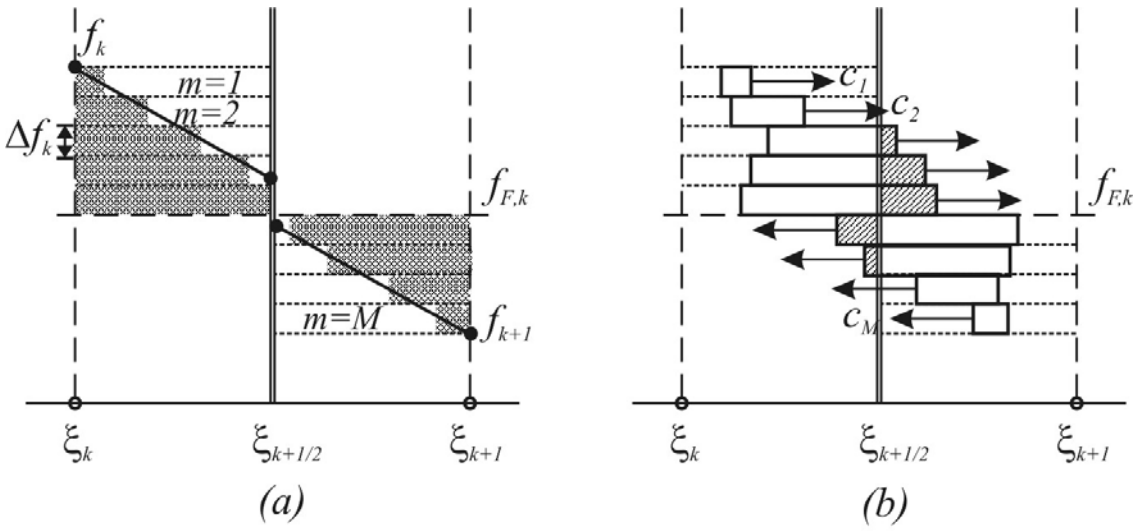

Figure 2. (a) Spline-function partition into small disturbance "bricks", background value determination; (b) "bricks" movement and integral flows computation.

For integral flow computation let find the linearized gas dynamic equation system solution. Assume that density, velocity and pressure functions are the sum of certain constant background values and small deviations:

$$\rho(\xi,t)=\overline{\rho}+\delta\rho(\xi,t),\quad v(\xi,t)=\overline{v}+\delta v(\xi,t),\quad p(\xi,t)=\overline{p}+\delta p(\xi,t) \tag{7}$$

here $\overline{\rho},\overline{v},\overline{p}$ =const, and the word "small" means that the following inequalities take place: $|\delta\rho/\overline{\rho}|\ll 1$, $|\delta v/\overline{v}|\ll 1$, $|\delta p/\overline{p}|\ll 1$. The same inequalities are assumed to be true not only for functions but for its derivatives. Also assume that the flow is adiabatic. In this case the number of gas dynamic equations in Lagrange coordinates decreases from three to two. After expressions (7) are substituted into the original system and addendums of second smallness order are neglected we obtain the linearized system where unknown variables are pressure and velocity small disturbances:

$$\begin{cases}\overline{\rho}\dfrac{\partial\delta v}{\partial t}+\dfrac{\partial\delta p}{\partial\xi}=0,\\ \dfrac{\partial\delta p}{\partial t}+\overline{\rho c}^2\dfrac{\partial\delta v}{\partial\xi}=0.\end{cases} \tag{8}$$

If the initial values $\delta\rho^0$, δv^0, δp^0 are known the general system solution is the superposition of two running waves:

$$\begin{cases}\delta v(\xi,t)=\dfrac{1}{2}\left(\delta v^0(\xi-\overline{c}t)+\dfrac{\delta p^0(\xi-\overline{c}t)}{\overline{\rho c}}+\delta v^0(\xi+\overline{c}t)-\dfrac{\delta p^0(\xi+\overline{c}t)}{\overline{\rho c}}\right),\\ \delta p(\xi,t)=\dfrac{\overline{\rho c}}{2}\left(\delta v^0(\xi-\overline{c}t)+\dfrac{\delta p^0(\xi-\overline{c}t)}{\overline{\rho c}}-\delta v^0(\xi+\overline{c}t)+\dfrac{\delta p^0(\xi+\overline{c}t)}{\overline{\rho c}}\right).\end{cases} \tag{9}$$

One can see from this expressions that in Lagrange coordinates the solution is always a sum of two addendums regardless what flow type takes place (subsonic, sonic or supersonic). One of this addendums moves with sound speed from the left to the right and the second moves from the right to the left. This fact simplifies integral flow computation algorithm as well as boundary condition formulation.

Let see how this facts can help with integral flow computation. During the time $\Delta t = t_{j+1} - t_j$ from $t=t_j$ to $t=t_{j+1}$ every small disturbance ("brick") $\delta\rho(x,t)$, $\delta u(x,t)$, $\delta p(x,t)$ disintegrates into Riemann waves. Each of these waves moves along its background accordingly to the linearized system solution (9). Movement speed of these "bricks" is equal to local sound speed. Note that the sound speed changes from level to level accordingly to the quasi-linearity features of gas dynamic equation system.

So the integral flows via the cut $\xi=\xi_{k+1/2}$ are formed with flows that are caused by common constant background and additional small disturbances level-by-level addendum. To find this addendum substitute expressions (7), (9) into integral flow formulas and transform them with the integral variable replacement:

$$\begin{cases} WQI^{j}_{k+\frac{1}{2}} = \overline{p}\Delta t + \int\limits_{\xi_{k+\frac{1}{2}}-\overline{c}\Delta t}^{\xi_{k+\frac{1}{2}}} \frac{\overline{\rho}}{2}\left(\delta v(\xi-\overline{c}t_j) + \frac{\delta p(\xi-\overline{c}t_j)}{\overline{\rho c}}\right)d\xi + \\ + \int\limits_{\xi_{k+\frac{1}{2}}}^{\xi_{k+\frac{1}{2}}+\overline{c}\Delta t} \frac{\overline{\rho}}{2}\left(-\delta v(\xi+\overline{c}t_j) + \frac{\delta p(\xi+\overline{c}t_j)}{\overline{\rho c}}\right)d\xi = \overline{p}\Delta t + \overrightarrow{\overline{WQI}}^{j}_{k+\frac{1}{2}} + \overleftarrow{\overline{WQI}}^{j}_{k+\frac{1}{2}}, \\ WUI^{j}_{k+\frac{1}{2}} = \overline{u}\Delta t + \int\limits_{\xi_{k+\frac{1}{2}}-\overline{c}\Delta t}^{\xi_{k+\frac{1}{2}}} \frac{1}{2\overline{c}}\left(\delta v(\xi-\overline{c}t_j) + \frac{\delta p(\xi-\overline{c}t_j)}{\overline{\rho c}}\right)d\xi + \\ + \int\limits_{\xi_{k+\frac{1}{2}}}^{\xi_{k+\frac{1}{2}}+\overline{c}\Delta t} \frac{1}{2\overline{c}}\left(\delta v(\xi+\overline{c}t_j) - \frac{\delta p(\xi+\overline{c}t_j)}{\overline{\rho c}}\right)d\xi = \overline{u}\Delta t + \overrightarrow{\overline{WUI}}^{j}_{k+\frac{1}{2}} + \overleftarrow{\overline{WUI}}^{j}_{k+\frac{1}{2}}, \\ WUI^{j}_{k+\frac{1}{2}} = \overline{p}\overline{u}\Delta t + \left(\overline{u}\overrightarrow{\overline{WQI}}^{j}_{k+\frac{1}{2}} + \overline{p}\overrightarrow{\overline{WUI}}^{j}_{k+\frac{1}{2}}\right) + \left(\overline{u}\overleftarrow{\overline{WQI}}^{j}_{k+\frac{1}{2}} + \overline{p}\overleftarrow{\overline{WUI}}^{j}_{k+\frac{1}{2}}\right). \end{cases} \quad (10)$$

Thus the integral flow computation is reduced to the calculation and summation of squares of those "brick" parts that cross cell boundary while moving to the border $\xi=\xi_{k+1/2}$ with its sound speed during the time Δt.

The stable condition directly ensues from the described algorithm of integral flow computation. The time step value Δt has to guarantee that no one "brick" moves out of the corresponding segment:

$$\max_k c_k^j \le \frac{h}{2}. \quad (11)$$

3.2 Two-dimensional problem features

The main difference between one- and two-dimensional problems is that the alternate directions method[4] is used instead of finding the strict solution of two-dimensional linearized system and double integral calculation. Accordingly the problem is reduced to one-dimensional case for each of two dimensional variables. The mesh function interpolation is implemented with the analogous two-dimensional local linear spline planes. For integral flows computation the obtained spline plane partition into three-dimensional "bricks" is also used.

3.3 Conversion Lagrange coordinates to Euler coordinates

The suggested algorithm is used as the first stage of gas dynamics equation system numerical solution by means of particle method. The idea is based on Harlow's PIC-method[7] (particle-in-cell method) and Belocerkovskiy's large particle method[8]. Both methods start with the solution of momentum and energy equations in Lagrange coordinates (without mass equation which is trivial in Lagrange coordinates). Then the obtained solution is recalculated with convective flow influence. Belocerkovskiy's large particle method permits to use suggested algorithm not only for the first Lagrange stage but also for the further solution conversation to Euler coordinates. The main value used in the second stage is the mass flow through cell boundary, i. e. $WVI^{j}_{k+1/2}$, that is determined in the first stage. This modification of original Belocerkovskiy's algorithm allows reducing the number of operations without precision fall.

3.4 Main properties of quasiacoustic scheme. Numerical experiment examples

Let's investigate the main properties of suggested gas dynamics equation system solution method (as a substantive problem) with the following example.

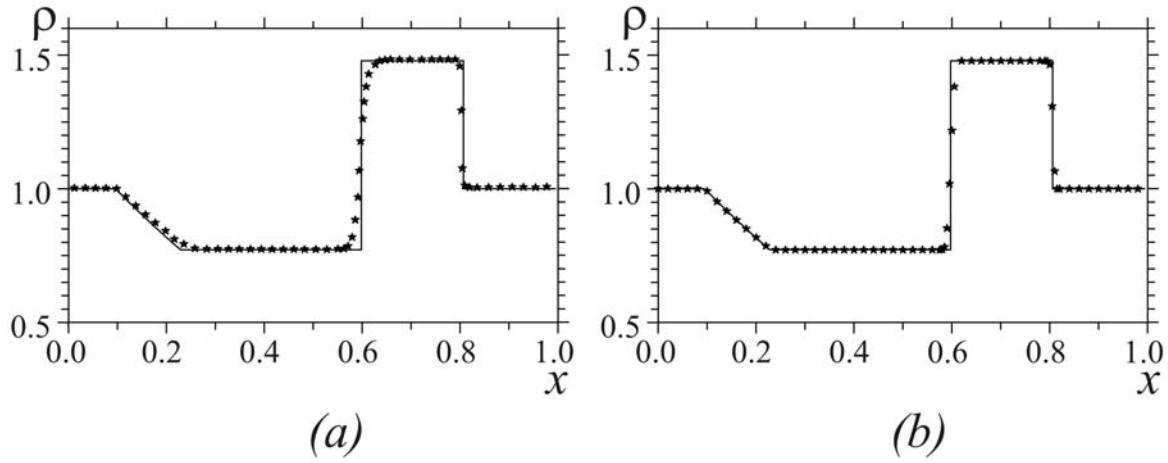

Figure 3. The solution to Sod's shock tube. Density plot of exact solution (solid line) and numerical solution (stars). The numerical solution is obtained with quasiacoustic scheme (a) and with Roe-Einfeldt-Osher's differential scheme (b).

In figure 3 (a) the numerical solution to Sod's shock tube specified by initial piecewise-constant gas state are displayed. In figure 3 (b) the solution of the same problem is obtained with Roe-Einfeldt-Osher's differential scheme[9,10] (the scheme with the increased approximation order). The grid consists of 200 cells. Every fourth point is displayed; in a vicinity of contact discontinuity and shock wave all points are shown.

The numerical solution and the exact benchmark solution are in good agreement. One can see that the solution obtained with constructed quasiacoustic scheme is monotonous. The contact discontinuity is captured worse than by Roe-Einfeldt-Osher's differential scheme. It is connected with the numerical dissipation originated because of the solution conversion to Euler coordinates. The shock front position is captured as accurately as with the increased approximation order scheme. The number of intervals on the shock front is equal to 3. Note that this solution is obtained without any limiters insertion (in contrast with Roe-Einfeldt-Osher's differential scheme). Furthermore, the quasiacoustic scheme has smaller pattern. Another quasiacoustic scheme advantage is time economy. It takes less labour expenditure for algorithm implementation and less time of its execution on computer than Roe-Einfeldt-Osher's differential scheme.

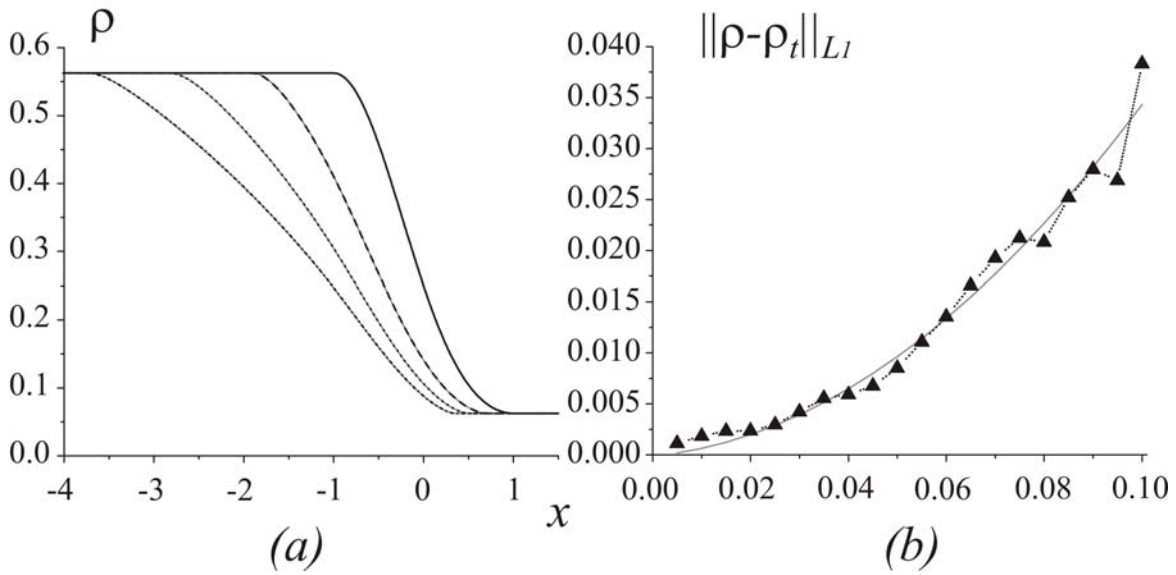

Figure 4. The numerical solution of problem with smooth initial profile. Density function at four consistent time moments (a) and the dependence between the solution error (norm L_1) and grid steps with constant Courant number (b).

The test problem with smooth solution helps to study the suggested original algorithm features (without the conversion to Euler coordinates). In figure 4 the numerical solution and the exact solution are displayed (a). There is also a graph of the dependence between the solution error and grid steps (b). The figure (b) shows that this dependence is nonlinear (error graph is approximated with parabola). This fact is in agreement with the a priori estimation[5]. Accordingly to this estimation the scheme has the approximation order on smooth solution above first.

3.5 Magnetic field diffusion equation solution

For the sake of stability the implicit differential scheme is used for the magnetic field diffusion equation solution:

$$\begin{cases} \dfrac{H_{i,j}^{k+1}-H_{i,j}^{k}}{\Delta t}+\dfrac{WX_{i+1/2,j}^{k+1}-WX_{i-1/2,j}^{k+1}}{h_x}+\dfrac{WY_{i,j+1/2}^{k+1}-WY_{i,j-1/2}^{k+1}}{h_y}=0, \\ \sigma_{i+1/2,j}WX_{i+1/2,j}^{k+1}=-\dfrac{c^2}{4\pi}\dfrac{H_{i+1,j}^{k+1}-H_{i,j}^{k+1}}{h_x}+\sigma_{i+1/2,j}\left(\overset{+}{u}_{i+1/2,j}H_{i,j}^{k+1}+\overset{-}{u}_{i+1/2,j}H_{i+1,j}^{k+1}\right), \\ \sigma_{i,j+1/2}WY_{i,j+1/2}^{k+1}=-\dfrac{c^2}{4\pi}\dfrac{H_{i,j+1}^{k+1}-H_{i,j}^{k+1}}{h_y}+\sigma_{i,j+1/2}\left(\overset{+}{v}_{i+1/2,j}H_{i,j}^{k+1}+\overset{-}{v}_{i+1/2,j}H_{i,j+1}^{k+1}\right) \end{cases} \quad (12)$$

(here $\overset{+}{u}_{i+1/2,j}=(u_{i+1/2,j}^{k}+|u_{i+1/2,j}^{k}|)/2$, $\overset{-}{u}_{i+1/2,j}=(u_{i+1/2,j}^{k}-|u_{i+1/2,j}^{k}|)/2$, the same expressions take place for *v*). The conductivity coefficient in nonperturbed gas flow is close or equals to zero. Because of this the alternate directions method[4] with data-flow variant of Thomas algorithm[11] is used for this equation solution.

3.6 The Lorentz force and Joule heating interaction

After all electromagnetic parameters computation the obtained gas velocity and internal energy values are recalculated with the Lorentz force and Joule heating interaction. Note that for stability reasons the implicit scheme is used to calculate the velocity rectifications determined by Lorentz force:

$$\begin{cases} \rho_{i,j}^{k+1}\dfrac{u_{i,j}^{k+1}-\tilde{u}_{i,j}^{k+1}}{\Delta t}=\sigma_{i,j}^{k+1}H_{i,j}^{k+1}\left(\dfrac{WX_{i+1/2,j}^{k+1}-WX_{i-1/2,j}^{k+1}}{2}-H_{i,j}^{k+1}u_{i,j}^{k+1}\right), \\ \rho_{i,j}^{k+1}\dfrac{v_{i,j}^{k+1}-\tilde{v}_{i,j}^{k+1}}{\Delta t}=\sigma_{i,j}^{k+1}H_{i,j}^{k+1}\left(\dfrac{WY_{i+1/2,j}^{k+1}-WY_{i-1/2,j}^{k+1}}{2}-H_{i,j}^{k+1}v_{i,j}^{k+1}\right) \end{cases} \quad (13)$$

(the tilde symbol is used for function values calculated on the previous gasdynamic stage). For internal energy rectifications determined by Joule heating traditional standard explicit scheme suits pretty well:

$$\begin{aligned} &\rho_{i,j}^{k+1}\frac{\varepsilon_{i,j}^{k+1}-\tilde{\varepsilon}_{i,j}^{k+1}}{\Delta t}=4\pi\sigma_{i,j}^{k+1}\left(\left(Ey_{i,j}^{k+1}\right)^2+\left(Ex_{i,j}^{k+1}\right)^2\right), \\ &Ey_{i+1/2,j}^{k+1}=WX_{i+1/2,j}^{k+1}-\overset{+}{u}_{i+1/2,j}H_{i,j}^{k+1}-\overset{-}{u}_{i+1/2,j}H_{i+1,j}^{k+1}, \\ &Ex_{i,j+1/2}^{k+1}=WY_{i,j+1/2}^{k+1}-\overset{+}{v}_{i,j+1/2}H_{i,j}^{k+1}-\overset{-}{v}_{i,j+1/2}H_{i,j+1}^{k+1}. \end{aligned} \quad (14)$$

4 THE NUMERICAL EXPERIMENT RESULTS

The numerical experiment results show that the T-layer forms and develops stable in gas with the initial parameters excess certain critical value. In the motion of initially two-

dimensional perturbation along the channel there arises a progressive transformation into one-dimensional flow structure. This transformation takes time required the perturbation to move along the channel axis a distance approximately equals to few perturbation lengths (fig. 5).

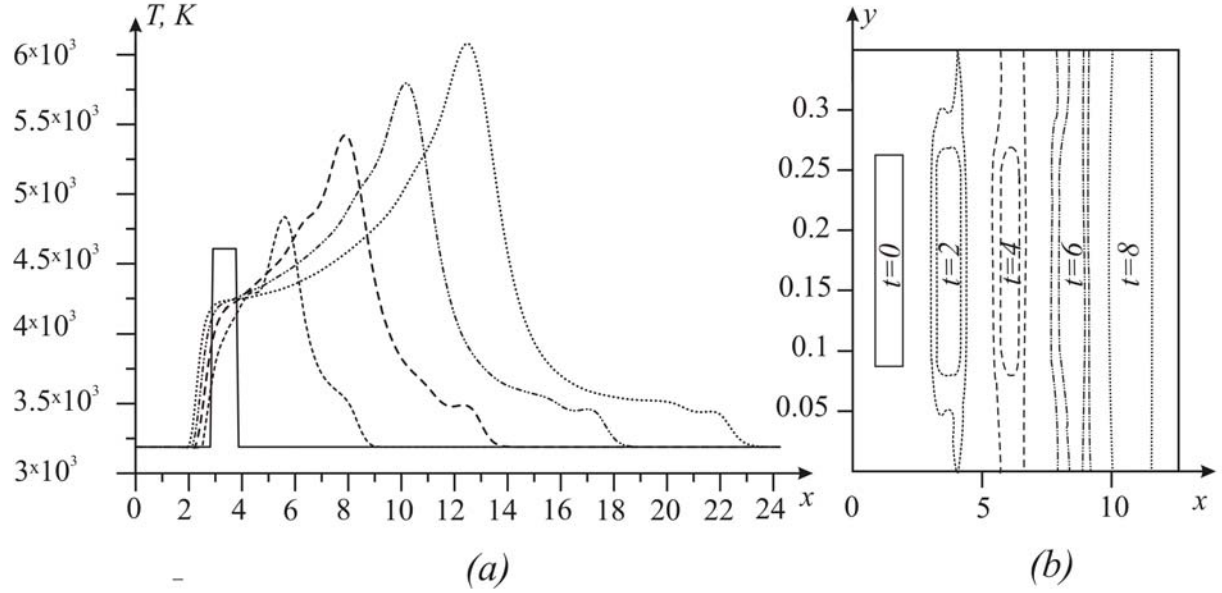

Figure 5. (a) Temperature profiles along channel axis at different time moments ($t_0=0$, $t_1=2\cdot10^{-3}$ sec, $t_2=4\cdot10^{-3}$ sec, $t_3=6\cdot10^{-3}$ sec, $t_4=8\cdot10^{-3}$ sec); (b) Temperature perturbation level lines at different time moments (time moments are the same as in fig. 5 (a)).

In figure 5 (a) the numerical experiment results of T-layer problem with $d/D=0,5$ are displayed. The plot shows that after a small temperature falling at the first time moment an intense temperature growth takes place. The maximum temperature value exceeds the initial perturbation temperature value soon. In figure 5 (b) temperature level lines are displayed. One can see that initially two-dimensional structure eventually transforms into one-dimensional structure.

The temperature increase rate depends on different parameters such as the perturbation initial temperature, the magnetic field value and the flow velocity. Perturbation longitudinal dimension also affects its evolution. Numerical experiment shows that the temperature increase remains with the perturbation width d decrease. However, the time for transformation initially two-dimensional structure into one-dimensional increases. The time required to exceed the initial perturbation temperature value also rises.

5 CONCLUSION

In the perturbing gas motion intensive Joule heating liberation arises. That leads to internal energy and pressure increase. Because of pressure rise the perturbation enlarges and compresses adjoining gas layers. That causes additional temperature elevation. This enlargement proceeds principally along y-direction. Therefore the flow gradually transforms to one-dimensional structure that is homogeneous along y-direction.

The numerical results confirm the proposition stated in work[12] about the possibility of T-layer nascence and evolution because of the corresponding process that initiates temperature

rise caused by Joule heating liberation. A number of parameters that significantly affect the T-layer nascence ability and evolution speed are detected.

To sum up, the main result of this work is the verification and confirmation of stated in work[12] T-layer nascence criterion in two-dimensional case. The T-layer arises if the magnetohydrodynamic interaction parameter $R_M=\sigma u l H^2/(2c^2 p)$ exceeds certain critical value depended on problem geometric parameters.

REFERENCES

[1] A.N. Tikhonov., A.A. Samarskiy, L.A. Zaklyazminskiy, P.P. Volosevich, L.M. Degtyaryov, S.P. Kurdyumov, U.P. Popov, V.S. Sokolov, A.P. Favorskiy. *Nonlinear effect of self-sustaining high-temperature conductive gas layer formation in nonstationary processes in magnetohydrodynamics*. DAN USSR, V.173, №4, 1967.

[2] N.V. Sosnin, A.P. Favorskiy. *Steady magnetohydrodynamic structures of T-layer* // Prepr. Keldysh Institute if Applied Mathematics. 1976. №64. 32 p.

[3] R.A. Volkova, A.V. Gulin, N.V. Sosnin, A.P. Favorskiy. *Numerical study for T-layer stability* // Prepr. Keldysh Institute if Applied Mathematics. 1975. №76. 19 p.

[4] A.A. Samarskiy. *Introdaction into theory of differential schemes*. -M.: Science, 1971. 553 p.

[5] M.V. Abakumov, A.M. Galanina, V.A. Isakov, N.N. Turina, A.P. Favorskiy, A.B. Khrulenko. *Quasiacoustic scheme for Euler gas dynamics equations* // Differential equations. 2011. V. 47 № 8. P. 1092-1098.

[6] V.M. Goloviznin, A.A. Samarskiy, A.P. Favorskiy. *Variation method of finite-difference mathematical models construction in hydrodynamic* // DAN USSA. 1977. V. 235. №6. P. 1285-1288.

[7] B. Older, S. Fernbakh, M. Rotenberg *Numerical methods in hydrodynamics.* -M.: Mir, 1967. - 385 p.

[8] O.M. Belocerkovskiy, U.M. Davidov. *Large particle method in gas dynamics*. -M.: Science. Main edition of physical and mathematical literatire. 1982. - 392 p.

[9] O.A. Kuznetsov. *Numerical study of Roe scheme with Einfeldt modification fro gas dynamics equations* // Prepr. Keldysh Institute if Applied Mathematics. 1998. №43. 44 p.

[10] M.P. Galanin, E.B.Savenkov. *Methods of mathematical models numerical analysis*. –M.: N. Bauman MSTU publishing office, 2010. -591 p.

[11] L.M. Degtyaryov, A.P. Favorskiy. *Data-flow variant of Thomas algorithm for tasks with strongly changink coefficients*. JVM MP, 1969. V. 9, №2. P. 211-218.

[12] L.M. Degtyaryov, L.A. Zaklyazminskiy, S.P. Kurdyumov, A.A. Samarskiy, V.S. Sokolov, A.P. Favorskiy. *Local finite conductivity perturbations evolution in small conductivity gas flow in magnetic field*. TVT, 1969. №9.

Received June 10, 2013